Cramer-Rao Bounds for Hybrid Localization Methods in LoS and NLoS Environments

Konstantinos Papakonstantinou and Dirk Slock
Mobile Communications Department
Eurecom Institute
Sophia Antipolis, France
Email: papakons@eurecom.fr, slock@eurecom.fr

***Abstract*—Performance bounds provide a solid theoretical ground for comparing different localization methods. Similarly to the actual performance, they depend on two factors, namely the accuracy of the available data that are used for localization and the geometry of the network. While the impact of the accuracy of the available data has been studied extensively, the literature on the impact of network geometry is still poor. Specifically only a limited number of papers examines hybrid methods and no paper considers NLoS environments. This contribution is a first attempt to fill this gap. Through straightforward derivations, meaningful expressions for the Cramer-Rao bounds of a Hybrid method are derived. Emphasis is given to the NLoS case, where the results reveal the scenarios under which the accuracy is low[1].**

I. Introduction

Traditional geometrical localization methods require estimates of one set of location dependent parameters (LDP) in a certain number of base stations (BS) that depends on the method. Two very common methods are the time-of-arrival (ToA) based and the angle-of-arrival or departure (AoA and AoD respectively) based. The former one uses the delays estimated in at least 3 BS (for 2-D scenarios) and performs trilateration to obtain the location of the mobile terminal (MT) while the latter one uses angles estimated in at least 2 BS and performs triangulation.

To overcome the need for a communication link between the MT and several BS and/or to be able to localize with high accuracy in multipath and non-line-of-sight (NLoS) environments, hybrid methods were introduced. In a hybrid method, different sets of LDP estimates are combined. Introducing more sets of LDP, some of which might come at the cost of extra nuisance parameters (eg. received signal strength might come at the cost of unknown path loss exponent), will lead to an enhancement in performance, as long as the total number of the newly introduced LDP is greater than the number of the extra nuisance parameters and the matrix of the partial derivatives of these LDP with respect to the nuisance parameters has full rank [1, Theorem 1].

In this contribution, we evaluate the performance of a ToA/AoA/AoD hybrid method in LoS and NLoS environments with 1 or more BS. To do so, we compute and plot the Cramer-Rao bound (CRB). In all geometrical localization methods, the CRB (and the actual performance) depends on two factors: the accuracy of the available LDP estimates and the network geometry. The impact of the accuracy of the available LDP estimates on the CRB has been studied extensively for both LoS and NLoS environments. For a NLoS environment that can be described by the single bounce model (SBM), it was first studied in [2]. However, in that contribution, the impact of network geometry on the accuracy of the hybrid method was completely omitted. As a matter of fact, to the best of the authors' knowledge, there exist no publications that address this topic. On the other hand, for LoS environments, there are many publications that deal with the impact of network geometry, especially for non-hybrid methods [3], [4], [5], [6]. For hybrid methods, the topic was studied in [7], [8].

In contrast to all of the aforementioned work, we derive expressions for the CRB as a function of distances and angles, which allow for easy interpretation of the impact of the network geometry. We do so, not only for the trivial case of a LoS environment, but also for a NLoS environment that can be described by the SBM. In the latter case, the location of the scatterers needs to be jointly estimated with the location of the MT, thus, from the CRB in its initial form (product of 3 matrices), it is impossible to understand the impact of network geometry. However, after a straightforward derivation, this becomes feasible. Finally, contour maps in the numerical examples' section, validate the conclusions drawn from the CRB expressions and serve as indicators on how the localization performance can be improved.

Notation: For any defined vector $\boldsymbol{a}$, $\boldsymbol{A} = diag\{\boldsymbol{a}\}$ and for any defined matrix $\boldsymbol{A}$, $\boldsymbol{a} = vec\{\boldsymbol{A}\}$. Extending this, a_i will denote the ith entry of $\boldsymbol{a}$ and the $\{i,i\}$ entry of $\boldsymbol{A}$. It therefore suffices to define any of the above (a vector, a diagonal matrix or just a scalar), to define all 3.

II. Channel Model

Let ϕ_i, ψ_i and d_i, $1 \leq i \leq N_s$, denote the AoA, AoD and length of the ith (N)LoS path respectively[2]. For a LoS

[1]Eurecom's research is partially supported by its industrial members: BMW Group Research & Technology, Bouygues Telecom, Cisco, Hitachi, ORANGE, SFR, Sharp, STMicroelectronics, Swisscom, Thales. The work presented in this paper has also been partially supported by the European FP7 projects Where and Newcom++.

[2]The length of the path is just the product of the speed of light times the corresponding estimated delay, thus we consider the path instead of the ToA.

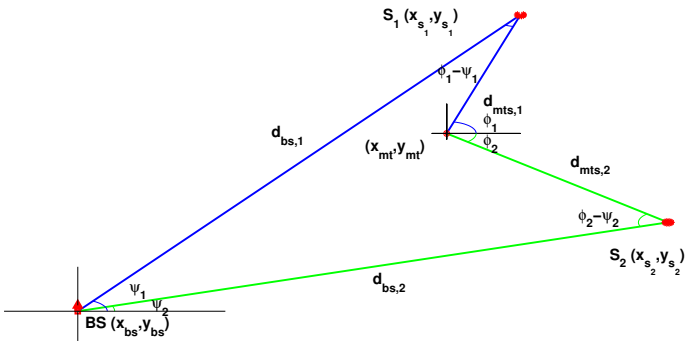

Fig. 1. Single Bounce model

environment, these LDP are equal to:

$$\phi_i = \frac{\pi}{2}(1 - sgn\{x_{mt} - x_{bs_i}\}) + \tan^{-1}\frac{y_{mt} - y_{bs_i}}{x_{mt} - x_{bs_i}} \quad (1)$$

$$\psi_i = \phi_i \pm \pi \quad (2)$$

$$d_i = \sqrt{(y_{bs_i} - y_{mt})^2 + (x_{bs_i} - x_{mt})^2}. \quad (3)$$

Based on the SBM we can also express these LDP explicitly as a function of the MT coordinates, x_{mt} and y_{mt}, for a NLoS environment:

$$\phi_i = \frac{\pi}{2}(1 - sgn\{x_{s_i} - x_{mt}\}) + \tan^{-1}\frac{y_{s_i} - y_{mt}}{x_{s_i} - x_{mt}} \quad (4)$$

$$\psi_i = \frac{\pi}{2}(1 - sgn\{x_{s_i} - x_{bs_i}\}) + \tan^{-1}\frac{y_{s_i} - y_{bs_i}}{x_{s_i} - x_{bs_i}} \quad (5)$$

$$d_i = d_{bs,i} + d_{mts,i} \quad (6)$$

where

$$d_{bs,i} = \sqrt{(y_{s_i} - y_{bs_i})^2 + (x_{s_i} - x_{bs_i})^2} \quad (7)$$

$$d_{mts,i} = \sqrt{(y_{s_i} - y_{mt})^2 + (x_{s_i} - x_{mt})^2} \quad . \quad (8)$$

SBM can describe accurately a NLoS environment, despite the fact that it is very simple. Its wide applicability stems from the fact that in a physical propagation environment, the more bounces, the larger the attenuation will be, not only because the scatterer absorbs some of the signals energy but also because more bounces usually implies a longer path length. Therefore, if a limited number of NLoS signal components with non-negligible energy arrive at the receiver, it is reasonable to assume that they have bounced only once.

III. CRB for LoS Environments

According to the CRB for an unbiased estimator $\hat{\mathbf{p}}$ of $\mathbf{p}$, the correlation matrix of the parameter estimation errors $\tilde{\mathbf{p}}$ is bounded below by the inverse of the Fisher Information Matrix (FIM), i.e.[3]:

$$R_{\tilde{\mathbf{p}}\tilde{\mathbf{p}}} = E\{(\hat{\mathbf{p}} - \mathbf{p})(\hat{\mathbf{p}} - \mathbf{p})^t\} \geq \mathbf{J}^{-1} \quad (9)$$

Let

$$\boldsymbol{\theta}_k = \begin{cases} \mathbf{d}, & k = 1 \\ \boldsymbol{\phi}, & k = 2 \\ \boldsymbol{\psi}, & k = 3 \end{cases} \quad (10)$$

[3]For matrices $\mathbf{A}$ and $\mathbf{B}$, $\mathbf{A} \geq \mathbf{B}$ means that $\mathbf{A} - \mathbf{B}$ is non-negative definite.

denote the vectors containing the LDP estimates[4].It is well known and can be easily shown, that the information contained in uncorrelated data (in our case LDP) can be summed up, so that the FIM for a hybrid localization method is given by:

$$\boldsymbol{J} = \sum_k \boldsymbol{J}_{\boldsymbol{\theta}_k} = \sum_k \frac{\partial \boldsymbol{\theta}_k^t}{\partial \mathbf{p}} \mathbf{C}_{\boldsymbol{\theta}_k}^{-1} \frac{\partial \boldsymbol{\theta}_k}{\partial \mathbf{p}^t} = \sum_k \frac{1}{\sigma_{\boldsymbol{\theta}_k}^2} \frac{\partial \boldsymbol{\theta}_k^t}{\partial \mathbf{p}} \frac{\partial \boldsymbol{\theta}_k}{\partial \mathbf{p}^t} \quad (11)$$

where the 3^{rd} equality holds only if the entries of $\boldsymbol{\theta}_k$, $\forall k$, are i.i.d. Gaussian with variance σ_k^2. To simplify analysis we will assume this to be true. If the AoA, AoD and delays have been jointly estimated, some correlation amongst them could be expected. This would lead to a different and more complicated FIM expression, due to the non-zero cross-covariance matrices. Since we are interested in studying solely the impact of the geometric configuration and not that of the LDP accuracy (and correlation), we consider this correlation to be weak and ignore it. Due to (2), it can be shown that

$$\sigma_{\boldsymbol{\phi}}^2 \boldsymbol{J}_{\boldsymbol{\phi}} = \sigma_{\boldsymbol{\psi}}^2 \boldsymbol{J}_{\boldsymbol{\psi}} \quad (12)$$

Therefore the FIM for this case becomes

$$\boldsymbol{J} = \frac{1}{\sigma_{\mathbf{d}}^2} \boldsymbol{J}_{\mathbf{d}} + \frac{1}{(\sigma_{\boldsymbol{\phi}}^2 + \sigma_{\boldsymbol{\psi}}^2)} \boldsymbol{J}_{\boldsymbol{\phi}} \quad (13)$$

Using eq. (1)-(3), we obtain for the 4 entries of the FIM

$$\mathbf{j}_{11} = \frac{N_s}{\sigma_d^2} - \sum_i \alpha_i \sin^2(\phi_i) \quad (14)$$

$$\mathbf{j}_{12} = \mathbf{j}_{21} = \sum_i \alpha_i \sin(\phi_i)\cos(\phi_i) \quad (15)$$

$$\mathbf{j}_{22} = \frac{N_s}{\sigma_d^2} - \sum_i \alpha_i \cos^2(\phi_i) \quad (16)$$

where

$$\alpha_i = \frac{1}{\sigma_d^2} - \frac{1}{(\sigma_\phi^2 + \sigma_\psi^2) d_i^2}. \quad (17)$$

The FIM for the LoS scenario is a 2×2 matrix and thus it can easily be inverted to get the CRB for the MT position CRB_{pos}. The derivation is simple and due to space limitation we give only the result below:

$$CRB_{pos} = tr\{\mathbf{J}^{-1}\} = \frac{tr\{\mathbf{J}\}}{det\{\mathbf{J}\}}$$

$$= \frac{2\sum_i \frac{1}{\sigma_d^2} - \frac{\alpha_i}{2}}{\left(\sum_i \frac{1}{\sigma_d^2} - \frac{\alpha_i}{2}\right)^2 - \left(\sum_i \frac{\alpha_i \cos 2\phi_i}{2}\right)^2 - \left(\sum_i \frac{\alpha_i \sin 2\phi_i}{2}\right)^2} \quad . \quad (18)$$

Introducing $\mathbf{C}_{2\phi} = diag\{\mathbf{c}_{2\phi}\}$, which follows the definitions of the vectors given in (27)-(28) and $\mathbf{A}$ we can rewrite the above formula to be able to compare it to the one for the NLoS case

$$CRB_{pos} = \frac{2\mathbf{1}^t(\frac{1}{\sigma_d^2}\mathbf{I} - \frac{1}{2}\mathbf{A})\mathbf{1}}{\frac{N_s}{\sigma_d^2}\mathbf{1}^t(\frac{1}{\sigma_d^2}\mathbf{I} - \mathbf{A})\mathbf{1} + \mathbf{1}^t\mathbf{A}(\mathbf{1}\mathbf{1}^t - \breve{\mathbf{C}}_{\delta 2\phi})\mathbf{A}\mathbf{1}} \quad (19)$$

where $\breve{\mathbf{C}}_{\delta 2\phi}$ is a symmetric matrix whose $\{i, j\}$ entry is equal to $cos(2\phi_i - 2\phi_j)$.

[4]For clarity, we omit $\hat{}$ on the LDP quantities, despite the fact that they are estimates.

IV. CRB for NLoS Environments

In a NLoS scenario, we are again interested in estimating the MT's coordinates, $\mathbf{p}_{int} = [x_{mt}, y_{mt}]^t$, but this time in the presence of nuisance parameters, which are the coordinates of the scatterers $\mathbf{p}_{nui} = [\mathbf{x}_s^t, \mathbf{y}_s^t]^t$. The set of all of the above $2N_s + 2$ parameters compose the vector:

$$\mathbf{p} = [\mathbf{p}_{int}^t, \mathbf{p}_{nui}^t]^t \tag{20}$$

To compute the CRB, the $(2N_s + 2) \times (2N_s + 2)$ FIM needs to be inverted. This is feasible even for large values of N_s, if we rewrite the FIM as a 2×2 block matrix and use blockwise inversion. Besides we only need to focus on the upper left 2×2 submatrix of its inverse, the trace of which gives the best possible accuracy, i.e. the CRB for the MT position.

$$CRB_{pos} = tr\{[\boldsymbol{J}^{-1}]_{1:2,1:2}\} \tag{21}$$

By substituting $\frac{\partial \boldsymbol{\theta}_k}{\partial \mathbf{p}^t} = [\frac{\partial \boldsymbol{\theta}_k}{\partial \mathbf{p}_{int}^t} \frac{\partial \boldsymbol{\theta}_k}{\partial \mathbf{p}_{nui}^t}]$ in (11), we get

$$\mathbf{J} = \begin{bmatrix} \sum_k \frac{1}{\sigma_{\dot{\theta}_k}^2} \frac{\partial \boldsymbol{\theta}_k^t}{\partial \mathbf{p}_{int}} \frac{\partial \boldsymbol{\theta}_k}{\partial \mathbf{p}_{int}^t} & \sum_k \frac{1}{\sigma_{\dot{\theta}_k}^2} \frac{\partial \boldsymbol{\theta}_k^t}{\partial \mathbf{p}_{int}} \frac{\partial \boldsymbol{\theta}_k}{\partial \mathbf{p}_{nui}^t} \\ \sum_k \frac{1}{\sigma_{\dot{\theta}_k}^2} \frac{\partial \boldsymbol{\theta}_k^t}{\partial \mathbf{p}_{nui}} \frac{\partial \boldsymbol{\theta}_k}{\partial \mathbf{p}_{int}^t} & \sum_k \frac{1}{\sigma_{\dot{\theta}_k}^2} \frac{\partial \boldsymbol{\theta}_k^t}{\partial \mathbf{p}_{nui}} \frac{\partial \boldsymbol{\theta}_k}{\partial \mathbf{p}_{nui}^t} \end{bmatrix} \triangleq \begin{bmatrix} \mathbf{J}_{11} & \mathbf{J}_{12} \\ \mathbf{J}_{21} & \mathbf{J}_{22} \end{bmatrix} \tag{22}$$

Using blockwise inversion we can obtain the upper left submatrix of the inverse of $\mathbf{J}$, given by the Schur complement of $\mathbf{J}_{22}$

$$[\mathbf{J}^{-1}]_{1:2,1:2} = (\mathbf{J}_{11} - \mathbf{J}_{12}\mathbf{J}_{22}^{-1}\mathbf{J}_{21})^{-1} \triangleq \mathbf{G}^{-1}. \tag{23}$$

The entries of $\mathbf{G}$ are given by eq. (62)-(64), in the appendix. The CRB for the position estimate is then given by

$$CRB_{pos} = tr\{\mathbf{G}^{-1}\} = \frac{tr\{\mathbf{G}\}}{det\{\mathbf{G}\}}$$
$$= \frac{2\mathbf{1}^t \bar{\mathbf{J}}_{det}^{-1} \mathbf{1}}{\mathbf{1}^t \bar{\mathbf{J}}_{det}^{-1} (\mathbf{Q}'_{\phi+\psi} \mathbf{1}\mathbf{1}^t \mathbf{Q}_{\phi+\psi} - \mathbf{S}_{\phi+\psi} \mathbf{1}\mathbf{1}^t \mathbf{S}_{\phi+\psi}) \bar{\mathbf{J}}_{det}^{-1} \mathbf{1}}$$
$$= \frac{2\mathbf{1}^t \bar{\mathbf{J}}_{det}^{-1} \mathbf{1}}{\mathbf{1}^t \bar{\mathbf{J}}_{det}^{-1} (\mathbf{1}\mathbf{1}^t - \breve{\mathbf{C}}_{\delta\phi+\delta\psi}) \bar{\mathbf{J}}_{det}^{-1} \mathbf{1}} \tag{24}$$

where $\breve{\mathbf{C}}_{\delta\phi+\delta\psi}$ is a symmetric matrix whose $\{i, j\}$ entry is equal to $cos(\phi_i - \phi_j + \psi_i - \psi_j)$ and the rest of the matrices are given in eq. (65)-(69) of the appendix.

V. The Impact of Network Geometry on the CRB

First lets observe from eq. (19) and (24) that both CRB depend on distances through the matrices $\mathbf{A}$ and $\bar{\mathbf{J}}_{det}$. This is no big surprise, since this hybrid method utilizes angles. In contrast to ToA-based methods where distances do not impact performance, in AoA methods, the greater the distances the signal components cover, the worse the performance. Similarly here, by taking the partial derivative of the LoS (NLoS) CRB with respect to any d_i ($d_{mts,i}$), it can be proved that performance worsens when the MT moves away from the BS (the scatterers). To demonstrate this, consider the following example, where the MT communicates with 2 BS. In all our examples, we consider the LDP variances to be constant. Their

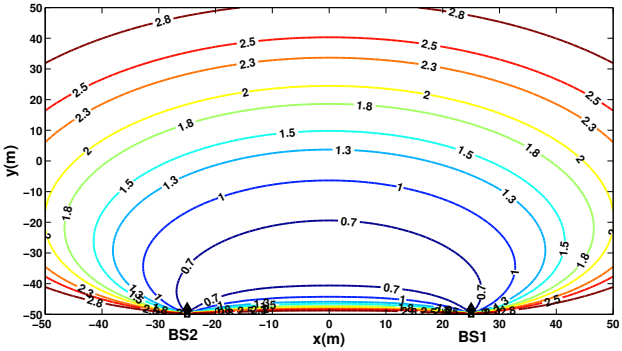

Fig. 2. LoS environment: CRB vs MT position

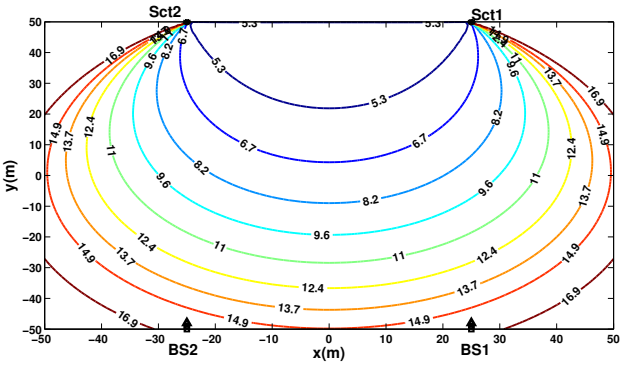

Fig. 3. NLoS environment: CRB vs MT position

values are $\sigma_d^2 = 25m$ and $\sigma_\phi^2 = \sigma_\psi^2 = 1^o$. The contour maps show the CRB for a region of $10^4 m^2$. The contour lines are based on the c.d.f. of the CRB. Numbering the lines in increasing order of the corresponding CRB, contour line j encloses $(j/10)100\%$, $j \in \{1, \ldots, 9\}$ of the total area, i.e., for a contour line j we have $p(CRB < CRB(j)) = j/10$. Therefore, these plots also give the circular error probable (CEP) [4] defined as the radius of the circle in which the estimate lies with probability P, eg. in fig. 2, the 90% CEP is $2.8m$. Another important remark can be made by observing the weighting factors of the distance matrices in eq. (65). These factors are the variances of the angles. If AoD is much more accurately estimated than AoA, i.e. if $\sigma_\psi^2 << \sigma_\phi^2$, then only the distances between the MT and the scatterers impact the performance. This was already observed in the numerical example illustrated in [9]. In that work, AoA is not known and thus assuming that the errors in all AoA are uniformly distributed in $[0\,, 360^o)$, $\sigma_\phi^2 > 10^3 >> 1 > \sigma_\psi^2$. The AoD/ToA/Doppler-Shift hybrid method proposed therein, has similar performance in pico-cells and macro-cells, because, if elliptical scattering model is considered for the former and circular for the latter, $\mathbf{d}_{mts}$ can be considered approximately the same (at least same order of magnitude), while $\mathbf{d}_{bs}$ is significantly different.

More interesting is the impact of the various angles. The NLoS CRB_{pos} depends solely on the sums and the differences of AoA with the corresponding AoD. This is no big surprise either, since due to symmetry in a 1 BS scenario, we would expect to obtain the same performance if we exchange the

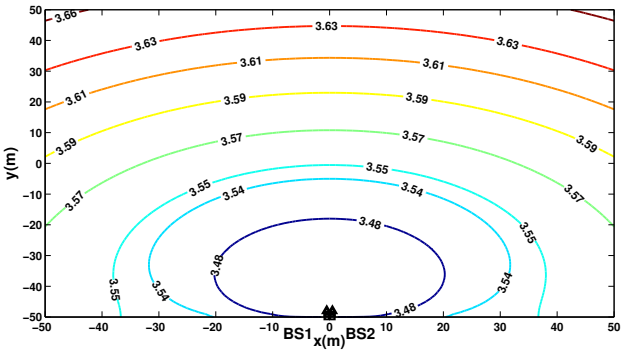

Fig. 4. LoS: CRB vs MT position for collocated BS

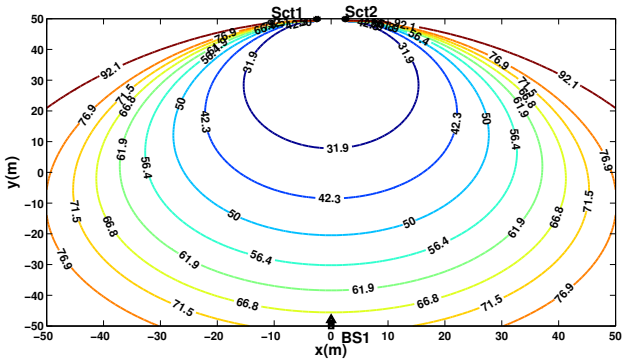

Fig. 5. NLoS: CRB vs MT position for collocated scatterers

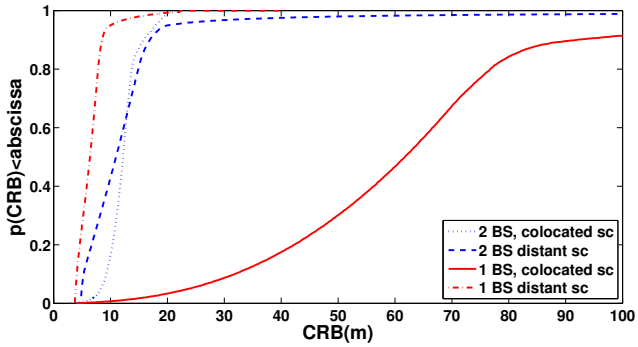

Fig. 6. c.d.f. of CRB for 4 NLoS scenarios

position of the BS with that of the MT. Furthermore, one can observe how similar the 2 CRB expressions are, by replacing ψ in the NLoS CRB_{pos}, using the LoS condition (2). The differences of AoA with AoD do not depend on the angles anymore and the sums are equal to two times the AoA plus a constant $c \in \{-2\pi, 0, 2\pi\}$ so that $\breve{\mathbf{C}}_{\delta\phi+\delta\psi} = \breve{\mathbf{C}}_{\delta 2\phi}$. One last important comment for the CRB final expressions concerns the matrices denoted by $\breve{\mathbf{C}}$. Due to the terms involving these matrices, the denominators decrease and thus the CRB increases. Both CRB are maximized with respect to angles if $\breve{\mathbf{C}}_{\delta 2\phi} = \breve{\mathbf{C}}_{\delta\phi+\delta\psi} = \mathbf{1}\mathbf{1}^t$. This corresponds to collocated BS for the LS case and collocated scatterers for the 1 BS NLoS case. While for the LoS the CRB remains finite(localization with this hybrid method is possible even with 1 BS), for the NLoS case the CRB goes to infinity and thus it is impossible to estimate the MT location. The significance of these matrices is demonstrated with the following contour maps for 1 and 2 BS scenarios. Comparing fig. (2) with fig. (4), we observe that indeed, in a LoS environment, performance decreases for closely located BS, but not significantly due to the first term in the denominator that depends only on distances. In fig. (5), we can observe the huge impact of collocated scatterers in a 1 BS environment. The CRB of this scenario is compared to that of fig. (3) and to the other two possible combinations (2 BS with collocated scatterers and 1 BS with distant scatterers) in fig.(6). It is shown that while for collocated scatterers it is preferable to have communications with more than 1 BS, in environments with distant scatterers communication with just 1 BS via multiple paths can sometimes lead to better performance.

VI. Conclusions

In this contribution we investigated the impact of network geometry and evaluated hybrid localization methods in both LoS and NLoS environments. We based our analysis on the single bounce model and derived meaningful expressions for the CRB in an attempt to explain how the actual location of the MT and the scatterers can affect the accuracy of the localization method. Comparison of the CRB using contour maps and c.d.f. plots for different scenarios, provided a graphical demonstration of the conclusions reached by interpreting the CRB expressions. The results presented herein are preliminary and could be extended in various directions, including investigating more scenarios, introducing dynamic instead of static channels, deriving and illustrating the optimal geometric configurations and comparing different hybrid methods.

Appendix

To compute the entries of $\mathbf{G}$ lets introduce some key quantities

$$\mathbf{D}_{mts} \triangleq ((\mathbf{Y}_s - y_{mt}\mathbf{I})^2 + (\mathbf{X}_s - x_{mt}\mathbf{I})^2)^{\frac{1}{2}} \quad (25)$$

$$\mathbf{D}_{bs} \triangleq ((\mathbf{Y}_s - \mathbf{Y}_{bs})^2 + (\mathbf{X}_s - \mathbf{X}_{bs})^2)^{\frac{1}{2}} \quad (26)$$

$$\mathbf{c}_{\boldsymbol{z}} \triangleq [\cos(z_1), \ldots, \cos(z_{Ns})]^t \quad (27)$$

$$\mathbf{s}_{\boldsymbol{z}} \triangleq [\sin(z_1), \ldots, \sin(z_{Ns})]^t \quad (28)$$

where the last two vectors are defined for any vector

$$\mathbf{z} = T(\boldsymbol{\phi}) + T(\boldsymbol{\psi}) \quad (29)$$

that is a linear transformation of the vectors containing AoA and AoD and thus contains angles. If the MT communicates only with 1 BS through a multipath environment, then $\mathbf{Y}_{bs} = y_{bs}\mathbf{I}$ and $\mathbf{X}_{bs} = x_{bs}\mathbf{I}$. Lets further define the vectors and matrices containing partial derivatives

$$\mathbf{D}_{\mathbf{x}_s} \triangleq \frac{\partial \mathbf{d}^t}{\partial \mathbf{x}_s} = \mathbf{C}_{\boldsymbol{\phi}} + \mathbf{C}_{\boldsymbol{\psi}} \quad (30)$$

$$\mathbf{D}_{\mathbf{y}_s} \triangleq \frac{\partial \mathbf{d}^t}{\partial \mathbf{y}_s} = \mathbf{S}_{\boldsymbol{\phi}} + \mathbf{S}_{\boldsymbol{\psi}} \quad (31)$$

$$\mathbf{d}_x^t \triangleq \frac{\partial \mathbf{d}^t}{\partial x_{mt}} = -\mathbf{c}_{\boldsymbol{\phi}}^t = -\mathbf{1}^t\mathbf{C}_{\boldsymbol{\phi}} \quad (32)$$

$$\mathbf{d}_y^t \triangleq \frac{\partial \mathbf{d}^t}{\partial y_{mt}} = -\mathbf{s}_{\boldsymbol{\phi}}^t = -\mathbf{1}^t\mathbf{S}_{\boldsymbol{\phi}} \quad (33)$$

$$\mathbf{\Phi}_{\mathbf{x}_s} \triangleq \frac{\partial \boldsymbol{\phi}^t}{\partial \mathbf{x}_s} = -\mathbf{S}_{\boldsymbol{\phi}}\mathbf{D}_{mts}^{-1} \quad (34)$$

$$\mathbf{\Phi}_{\mathbf{y}_s} \triangleq \frac{\partial \boldsymbol{\phi}^t}{\partial \mathbf{y}_s} = \mathbf{C}_{\boldsymbol{\phi}}\mathbf{D}_{mts}^{-1} \quad (35)$$

$$\boldsymbol{\phi}_x^t \triangleq \frac{\partial \boldsymbol{\phi}^t}{\partial x_{mt}} = \mathbf{s}_{\boldsymbol{\phi}}^t\mathbf{D}_{mts}^{-1} = \mathbf{1}^t\mathbf{S}_{\boldsymbol{\phi}}\mathbf{D}_{mts}^{-1} \quad (36)$$

$$\boldsymbol{\phi}_y^t \triangleq \frac{\partial \boldsymbol{\phi}^t}{\partial y_{mt}} = -\mathbf{c}_{\boldsymbol{\phi}}^t\mathbf{D}_{mts}^{-1} = -\mathbf{1}^t\mathbf{C}_{\boldsymbol{\phi}}\mathbf{D}_{mts}^{-1} \quad (37)$$

$$\mathbf{\Psi}_{\mathbf{x}_s} \triangleq \frac{\partial \boldsymbol{\psi}^t}{\partial \mathbf{x}_s} = -\mathbf{S}_{\boldsymbol{\psi}}\mathbf{D}_{bs}^{-1} \quad (38)$$

$$\mathbf{\Psi}_{\mathbf{y}_s} \triangleq \frac{\partial \boldsymbol{\psi}^t}{\partial \mathbf{y}_s} = \mathbf{C}_{\boldsymbol{\psi}}\mathbf{D}_{bs}^{-1} \quad (39)$$

$$\boldsymbol{\psi}_x^t \triangleq \frac{\partial \boldsymbol{\psi}^t}{\partial x_{mt}} = \mathbf{0}^t \quad (40)$$

$$\boldsymbol{\psi}_x^t \triangleq \frac{\partial \boldsymbol{\psi}^t}{\partial y_{mt}} = \mathbf{0}^t \quad . \quad (41)$$

Based on this we can compute each of the submatrices in (23). $\mathbf{J}_{22}$ is a 2×2 block matrix, each $N_s \times N_s$ submatrix of which is diagonal as long as the paths are distinct. Thus, we can again use block inversion and the solution is very simple since it resembles the solution of the 2×2 matrix inversion problem. Let

$$\mathbf{J}_{22} = \begin{bmatrix} \mathbf{J}_{22a} & \mathbf{J}_{22b} \\ \mathbf{J}_{22b} & \mathbf{J}_{22d} \end{bmatrix}. \quad (42)$$

Then

$$\mathbf{J}_{22}^{-1} = \begin{bmatrix} \mathbf{J}_{22d}\mathbf{J}_{det}^{-1} & -\mathbf{J}_{22b}\mathbf{J}_{det}^{-1} \\ -\mathbf{J}_{22b}\mathbf{J}_{det}^{-1} & \mathbf{J}_{22a}\mathbf{J}_{det}^{-1} \end{bmatrix} \quad (43)$$

where $\mathbf{J}_{det} = \mathbf{J}_{22a}\mathbf{J}_{22d} - \mathbf{J}_{22b}^2$ and the 3 different submatrices composing $\mathbf{J}_{22}$ are given by:

$$\mathbf{J}_{22a} = \sigma_d^{-2}\mathbf{D}_{\mathbf{x}_s}^2 + \sigma_\phi^{-2}\mathbf{\Phi}_{\mathbf{x}_s}^2 + \sigma_\psi^{-2}\mathbf{\Psi}_{\mathbf{x}_s}^2 \quad (44)$$

$$\mathbf{J}_{22b} = \sigma_d^{-2}\mathbf{D}_{\mathbf{x}_s}\mathbf{D}_{\mathbf{y}_s} + \sigma_\phi^{-2}\mathbf{\Phi}_{\mathbf{x}_s}\mathbf{\Phi}_{\mathbf{y}_s} + \sigma_\psi^{-2}\mathbf{\Psi}_{\mathbf{x}_s}\mathbf{\Psi}_{\mathbf{y}_s} \quad (45)$$

$$\mathbf{J}_{22d} = \sigma_d^{-2}\mathbf{D}_{\mathbf{y}_s}^2 + \sigma_\phi^{-2}\mathbf{\Phi}_{\mathbf{y}_s}^2 + \sigma_\psi^{-2}\mathbf{\Psi}_{\mathbf{y}_s}^2 \quad (46)$$

$\mathbf{J}_{21} = \mathbf{J}_{12}^t$ can also be expressed as a 2×2 block matrix

$$\mathbf{J}_{21} = \begin{bmatrix} \mathbf{j}_{21a} & \mathbf{j}_{22b} \\ \mathbf{j}_{22c} & \mathbf{j}_{22d} \end{bmatrix}. \quad (47)$$

The elements of this block matrix are the following vectors

$$\mathbf{j}_{12a} = \sigma_d^{-2}\mathbf{D}_{\mathbf{x}_s}\mathbf{d}_x + \sigma_\phi^{-2}\mathbf{\Phi}_{\mathbf{x}_s}\boldsymbol{\phi}_x \quad (48)$$

$$\mathbf{j}_{12b} = \sigma_d^{-2}\mathbf{D}_{\mathbf{y}_s}\mathbf{d}_x + \sigma_\phi^{-2}\mathbf{\Phi}_{\mathbf{y}_s}\boldsymbol{\phi}_x \quad (49)$$

$$\mathbf{j}_{12c} = \sigma_d^{-2}\mathbf{D}_{\mathbf{x}_s}\mathbf{d}_y + \sigma_\phi^{-2}\mathbf{\Phi}_{\mathbf{x}_s}\boldsymbol{\phi}_y \quad (50)$$

$$\mathbf{j}_{12d} = \sigma_d^{-2}\mathbf{D}_{\mathbf{y}_s}\mathbf{d}_y + \sigma_\phi^{-2}\mathbf{\Phi}_{\mathbf{y}_s}\boldsymbol{\phi}_y \quad (51)$$

Last,

$$\mathbf{J}_{11} = \begin{bmatrix} \sigma_d^{-2}\mathbf{d}_x^t\mathbf{d}_x + \sigma_\phi^{-2}\boldsymbol{\phi}_x^t\boldsymbol{\phi}_x & \sigma_d^{-2}\mathbf{d}_x^t\mathbf{d}_y + \sigma_\phi^{-2}\boldsymbol{\phi}_x^t\boldsymbol{\phi}_y \\ \sigma_d^{-2}\mathbf{d}_x^t\mathbf{d}_y + \sigma_\phi^{-2}\boldsymbol{\phi}_x^t\boldsymbol{\phi}_y & \sigma_d^{-2}\mathbf{d}_y^t\mathbf{d}_y + \sigma_\phi^{-2}\boldsymbol{\phi}_y^t\boldsymbol{\phi}_y \end{bmatrix}. \quad (52)$$

Substituting the 4 submatrices given by (43),(47),(52) into (23) we obtain after some algebraic computations the 4 entries of $\mathbf{G}$:

$$g_{11} = \mathbf{d}_x^t\mathbf{F}_D\mathbf{d}_x + \boldsymbol{\phi}_x^t\mathbf{F}_\Phi\boldsymbol{\phi}_x + 2\mathbf{d}_x^t\mathbf{F}\boldsymbol{\phi}_x \quad (53)$$

$$g_{22} = \mathbf{d}_y^t\mathbf{F}_D\mathbf{d}_y + \boldsymbol{\phi}_y^t\mathbf{F}_\Phi\boldsymbol{\phi}_y + 2\mathbf{d}_y^t\mathbf{F}\boldsymbol{\phi}_y \quad (54)$$

$$g_{21} = g_{12} = \mathbf{d}_x^t\mathbf{F}_D\mathbf{d}_y + \boldsymbol{\phi}_x^t\mathbf{F}_\Phi\boldsymbol{\phi}_y + \mathbf{d}_x^t\mathbf{F}\boldsymbol{\phi}_y + \mathbf{d}_y^t\mathbf{F}\boldsymbol{\phi}_x \quad (55)$$

where we have introduced the matrices

$$\mathbf{F}_D = \sigma_d^{-2}\mathbf{I} - \sigma_d^{-4}\left(\mathbf{D}_{\mathbf{x}_s}^2\mathbf{J}_{22a} + \mathbf{D}_{\mathbf{y}_s}^2\mathbf{J}_{22d} - 2\mathbf{D}_{\mathbf{x}_s}\mathbf{D}_{\mathbf{y}_s}\mathbf{J}_{22b}\right)\mathbf{J}_{det}^{-1} \quad (56)$$

$$\mathbf{F}_\Phi = \sigma_\phi^{-2}\mathbf{I} - \sigma_\phi^{-4}\left(\mathbf{\Phi}_{\mathbf{x}_s}^2\mathbf{J}_{22a} + \mathbf{\Phi}_{\mathbf{y}_s}^2\mathbf{J}_{22d} - 2\mathbf{\Phi}_{\mathbf{x}_s}\mathbf{\Phi}_{\mathbf{y}_s}\mathbf{J}_{22b}\right)\mathbf{J}_{det}^{-1} \quad (57)$$

$$\mathbf{F} = -\sigma_d^{-2}\sigma_\phi^{-2}\left(\mathbf{D}_{\mathbf{x}_s}\mathbf{\Phi}_{\mathbf{x}_s}\mathbf{J}_{22a} + \mathbf{D}_{\mathbf{y}_s}\mathbf{\Phi}_{\mathbf{y}_s}\mathbf{J}_{22d} - (\mathbf{D}_{\mathbf{x}_s}\mathbf{\Phi}_{\mathbf{y}_s} + \mathbf{D}_{\mathbf{y}_s}\mathbf{\Phi}_{\mathbf{x}_s})\mathbf{J}_{22b}\right)\mathbf{J}_{det}^{-1} \quad (58)$$

Replacing the vectors that contain partial derivatives into the entries of $\mathbf{G}$, we obtain

$$g_{11} = \mathbf{1}^t(\mathbf{C}_{\boldsymbol{\phi}}^2\mathbf{F}_D + \mathbf{D}_{mts}^{-2}\mathbf{S}_{\boldsymbol{\phi}}^2\mathbf{F}_\Phi - 2\mathbf{D}_{mts}^{-1}\mathbf{C}_{\boldsymbol{\phi}}\mathbf{S}_{\boldsymbol{\phi}}\mathbf{F})\mathbf{1} \quad (59)$$

$$g_{22} = \mathbf{1}^t(\mathbf{S}_{\boldsymbol{\phi}}^2\mathbf{F}_D + \mathbf{D}_{mts}^{-2}\mathbf{C}_{\boldsymbol{\phi}}^2\mathbf{F}_\Phi + 2\mathbf{D}_{mts}^{-1}\mathbf{C}_{\boldsymbol{\phi}}\mathbf{S}_{\boldsymbol{\phi}}\mathbf{F})\mathbf{1} \quad (60)$$

$$g_{12} = \mathbf{1}^t\big(\mathbf{C}_{\boldsymbol{\phi}}\mathbf{S}_{\boldsymbol{\phi}}\mathbf{F}_D - \mathbf{D}_{mts}^{-2}\mathbf{C}_{\boldsymbol{\phi}}\mathbf{S}_{\boldsymbol{\phi}}\mathbf{F}_\Phi + \mathbf{D}_{mts}^{-1}(\mathbf{C}_{\boldsymbol{\phi}}^2 - \mathbf{S}_{\boldsymbol{\phi}}^2)\mathbf{F}\big)\mathbf{1} \quad (61)$$

Finally, replacing the matrices that contain the partial derivatives from (30)-(39) into the submatrices of $\mathbf{J}_{22}$ and the matrices $\mathbf{F}$, $\mathbf{F}_\Phi$, $\mathbf{F}_D$ and subsequently the results into the entries of $\mathbf{G}$, we obtain

$$g_{11} = \mathbf{1}^t(\mathbf{Q}'_{\boldsymbol{\phi}+\boldsymbol{\psi}}\bar{\mathbf{J}}_{det}^{-1})\mathbf{1} \quad (62)$$

$$g_{22} = \mathbf{1}^t(\mathbf{Q}_{\boldsymbol{\phi}+\boldsymbol{\psi}}\bar{\mathbf{J}}_{det}^{-1})\mathbf{1} \quad (63)$$

$$g_{12} = -\mathbf{1}^t(\mathbf{S}_{\boldsymbol{\phi}+\boldsymbol{\psi}}\bar{\mathbf{J}}_{det}^{-1})\mathbf{1} \quad (64)$$

where

$$\bar{\mathbf{J}}_{det} = (\sigma_d^2\sigma_\phi^2\sigma_\psi^2)\mathbf{D}_{bs}^2\mathbf{D}_{mts}^2\mathbf{C}_I^{-1}\mathbf{J}_{det} = ((\sigma_\psi^2\mathbf{D}_{bs}^2 + \sigma_\phi^2\mathbf{D}_{mts}^2)\mathbf{Q}_{\boldsymbol{\phi}-\boldsymbol{\psi}} + \sigma_d^2\mathbf{Q}'_{\boldsymbol{\phi}-\boldsymbol{\psi}}) \quad (65)$$

and we have introduced

$$\mathbf{Q}_{\boldsymbol{\phi}-\boldsymbol{\psi}} = \mathbf{I} + \mathbf{C}_{\boldsymbol{\phi}-\boldsymbol{\psi}} \quad (66)$$

$$\mathbf{Q}'_{\boldsymbol{\phi}-\boldsymbol{\psi}} = \mathbf{I} - \mathbf{C}_{\boldsymbol{\phi}-\boldsymbol{\psi}} \quad (67)$$

$$\mathbf{Q}_{\boldsymbol{\phi}+\boldsymbol{\psi}} = \mathbf{I} + \mathbf{C}_{\boldsymbol{\phi}+\boldsymbol{\psi}} \quad (68)$$

$$\mathbf{Q}'_{\boldsymbol{\phi}+\boldsymbol{\psi}} = \mathbf{I} - \mathbf{C}_{\boldsymbol{\phi}+\boldsymbol{\psi}} \quad . \quad (69)$$

REFERENCES

[1] K. Papakonstantinou and D. Slock, "Identifiability and Performance Concerns in Location Estimation," 2009, proc. IEEE International Conference on Acoustics, Speech and Signal Processing 2009.

[2] H. Miao, K. Yu, and M. J. Juntti, "Positioning for NLOS Propagation: Algorithm Derivations and Cramer-Rao Bounds," *IEEE Trans. Veh. Technol.*, vol. 56, no. 5, pp. 2568 – 2580, 2007.

[3] W. H. Foy, "Position-location Solutions by Taylor-Series Estimation," *IEEE Trans. Aerosp. Electron. Syst.*, vol. 12, no. 2, pp. 187 – 194, 1976.

[4] D. J. Torrieri, "Statistical Theory of Passive Location Systems," *IEEE Trans. Aerosp. Electron. Syst.*, vol. 20, no. 2, pp. 183 – 198, 1984.

[5] N. Levanon, "Lowest GDOP in 2-D Scenarios," *IEE Radar, Sonar and Navigation*, vol. 147, no. 3, pp. 149 – 155, 2000.

[6] M. Spirito, "On the Accuracy of Cellular Mobile Station Location Estimation," *IEEE Trans. Veh. Technol.*, vol. 50, no. 3, pp. 674 – 685, 2001.

[7] C. Fritsche and A. Klein, "Cramer-Rao Lower Bounds for Hybrid Localization of Mobile Terminals," in *Proc. 5th Workshop on Positioning, Navigation and Communication*, Mar. 2008.

[8] M. Laaraiedh, S. Avrillon, and B. Uguen, "Hybrid Data Fusion Techniques for Localization in UWB Networks," in *Proc. 6th Workshop on Positioning, Navigation and Communication*, Mar. 2009.

[9] K. Papakonstantinou and D. Slock, "Hybrid TOA/AOD/Doppler-Shift Localization Algorithm for NLOS Environments," in *Proc. IEEE 20th Personal, Indoor and Mobile Radio Communications Symposium (PIMRC)*, 2009.